GENERAL

INTRODUCTION

"There's Plenty of Room at the Bottom"

Richard Phillips Feynman's talk delivered at the annual American Physical Society meeting, Caltech in 1959 [1] was an invitation to enter a new field of "nanotechnology", and later on became inspiration for the conceptual foundations of nanotechnology.

The term "nano" is derived from the Greek *nánnos* (Latin, *nanus*), meaning dwarf.

Scientific story of Nanotechnology

In 1857, Michael Faraday reported the synthesis of colloidal solution of Au nanoparticles (Au NPs), "activated gold", during his addressed at the Royal Society of London. With a purple color slide, he stated that it contained "Gold reduced in exceedingly fine particles, which becoming diffused, produce a ruby red fluid, the various preparations of gold, whether ruby, green, violet or blue consist of that substance in a metallic divided state" [2]. He also postulated exactly about the physical state of colloids and explains how the color of gold colloid changes on adding common salt (NaCl). Faraday is considered as the first researcher into nanoscience and nanotechnology because of his remarkable discovery of Faraday–Tyndall effect due to scattering of light by colloidal particles.

In 1959, the American scientist Richard Feynman delivered a famous visionary lecture in which he stated that "The principles of physics, as far as I can see, do not speak against the possibility of maneuvering things atom by atom [1]." This later paved the way for nanotechnology. At that time, Feynman's words were considered as conceptual and science fiction because nanomaterials were mostly unexplored due to technical difficulties. This lecture is referred to be the origin of nanotechnological paradigm.

In 1974, the Japanese scientist, Norio Taniguchi was first to use the term "nano-technology" in a conference [3], to describe the semiconductor processes such as thin film deposition and ion beam milling exhibiting characteristic control on the order of a nanometer. His definition was, "'Nano-technology' mainly consists of the processing of, separation, consolidation, and deformation of materials by one atom or one molecule." However, the term was untouched again until 1981.

In 1981, the American scientist, Eric Drexler, who was unaware of Taniguchi's prior use of the term, published his paper on, “Molecular Engineering: An approach to the development of general capabilities for molecular manipulation [4],” which popularized the concept of nanotechnology and founded the field of molecular nanotechnology. The insight ideas on nanotechnology were further developed by Drexler and published as a book in 1986, “*Engines of Creation*” [5]. He envisioned a molecular nanotechnology discipline, using bottom-up approach for the fabrication of products with increased molecular control. The constructed system using this technique was clean, efficient, and highly productive, which generated an enormous impact on the further development of nanotechnology.

The discovery of scanning probe microscopy in 1986, allowed the scientists to see individual atoms for the first time and this boosted the nanotechnology findings rapidly. In 1990, the scientists of IBM succeeded in moving xenon atoms to create the “IBM Logo” over the tip of a scanning tunneling microscope (CNET, IBM’s 35 atoms and the rise of nanotech).

In 1991, the Japanese physicist, Sumio Iijima discovered carbon nanotube (CNT) and shared the Kavli Prize in nanoscience. CNTs, like buckyballs, are entirely composed of carbon, but in a tubular shape. They exhibit extraordinary properties in terms of strength, electrical, and thermal conductivity among others [6]. In 1992, American chemist, Moungi Bawendi [7] invented a method for controlled synthesis of quantum dots nanocrystals, which is used for number of applications ranging from computing to biology to high-efficiency photovoltaics and many more.

In 2005, the American scientist, James Tour [8], invented directional control thermally driven Single-Molecule Nanocars (nanoscale car) made of oligo (phenylene ethynylene) with alkynyl axles and four spherical C60 fullerenes (buckyball) wheels.

After these breakthroughs, nanotechnology paved the way and numbers of articles and patents are published each year, even today and dominantly becomes the most impactful technology of the time.

What are Nanomaterials?

Nanomaterials are defined as a set of substances where at least one dimension is between the range of 1-100 nanometers. A nanometer is the billionth part of a meter - approximately 1,00,000 times smaller than the diameter of a human hair. For better understanding of nano size, comparison of different materials is shown in figure 1.

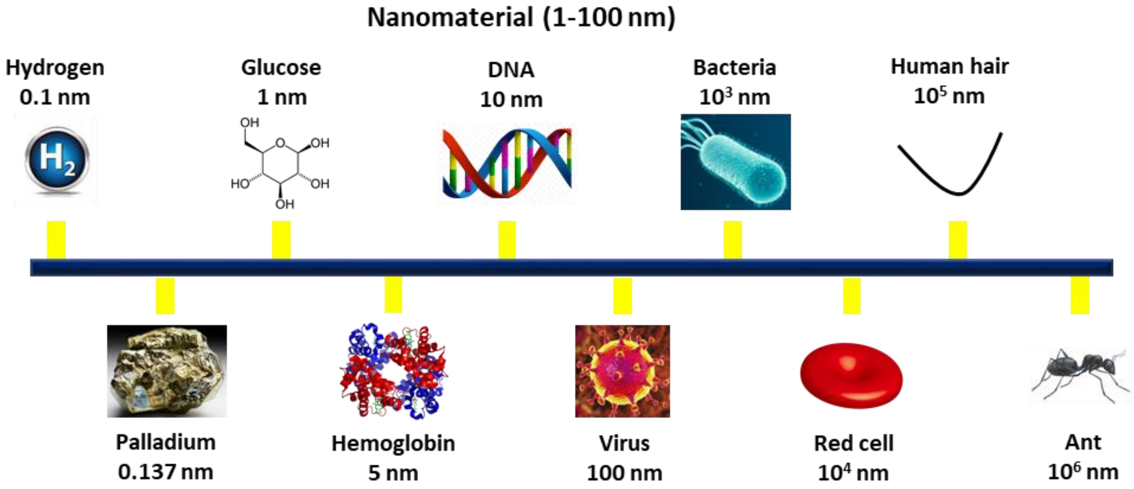

Figure 1 Comparison of nanomaterials size.

Properties of nanomaterials

The nanomaterials with the critical size (<100 nm) show unique and fascinating properties.

The *excitation, emission, chemical reactivity and stability* are size-dependent properties at nano-regime. Not only size, the shape also plays an important role in judging the nanomaterial properties [9]. The properties of nanomaterials can be tuned by controlling the size, during their synthesis by using different methods.

Catalytic properties: The activity of nanocatalysts, especially in heterogeneous reactions is mainly depends on the shape and size of active species deposited onto the support, as only surface metal atoms take part in a chemical reaction [37–39]. In general, on decreasing the particle size the number of particles on the surface increases, ultimately enhances the surface area to volume ratio (SA/V), which is responsible for high catalytic efficiency of the catalyst. The coordination number for surface atoms is less than the inner atoms and so they mobile easily. Based on this phenomenon, by surface modification, one can tune the catalytic properties of the nanomaterials.

Electronic properties of nanomaterials are based on their electronic band structure, which is the function of particle size. The molecular state consists the delocalized bands whereas in nanocrystal, the band structure is in between the discrete states of atoms and continuous bands of crystals. These adjacent molecular orbitals energy separation depends on the size of the particle, on increasing the size, the separation of energy levels decreases whereas the metallic character increases and as a result, gradually semiconductor nature increases [10].

Magnetic properties of different types like dia, para, ferro, anti-ferro and ferrimagnetic properties of bulk material can be tuned at nanoscale. The soft materials have low coercivity with small hysteresis area and these materials can be magnetized by a low magnetic field whereas, the hard magnets are contrasted to this. The coercivity is dependent on the particle size and generally, on increasing the surface area the coercivity and saturation magnetization increases. Hence, the nanomaterials have more surface area with less grain size and show high magnetic strength. With further decrease in particle size, the ferromagnetic property changes to paramagnetic. These paramagnetic materials behave in a different way from the bulk material which is known as superparamagnetic. The magnetic materials can be applicable in data storage capacity, electronic circuits, actuators, transformers, power generators and many more [9].

Optical properties: The interaction with light, is governed by size, shape, doping, surface characteristics and surrounding environment. This property is due to their surface plasmon and quantum confinement of electrons. Free electron density and dielectric medium of nanomaterial will judge the surface plasmon resonance energy. The optical properties can be tuned greatly by particle size, for instance, 2.3 nm size CdSe emits blue light whereas 5.5 nm size CdSe emits red light. Based on the optical properties, nanomaterials can be used in polymers to increase their refractive index for better resolution images development in LCD's and LED's [11].

Classification of Nanomaterials

According to Siegel [12], nanostructured materials are classified as three dimensional, two dimensional, one dimensional and zero dimensional nanostructures (Figure 2).

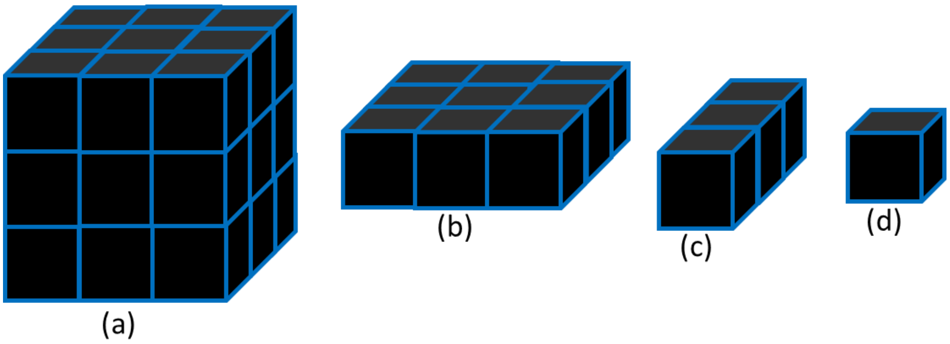

Figure 2 (a) 3D nanomaterial, (b) 2D nanomaterial, (c) 1D nanomaterial and (d) 0D nanomaterial.

Applications of Nanomaterials

It is evident that nanomaterials better their conventional counterparts because of their superior chemical, physical and mechanical properties and their exceptional formability. As a result, they have been known to showcase a variety of applications including, but not limited to, those listed below.

- Next-generation computer chips
- Kinetic energy penetrators with improved lethality
- Better insulation materials
- Phosphors for high-definition TV
- Low-cost flat-panel displays
- Tougher and harder cutting tools
- Elimination of pollutants
- High energy density batteries and electronics
- High-power magnets
- High-sensitivity sensors
- Automobiles with greater fuel efficiency
- Better future weapons platforms
- Longer-lasting satellites
- Longer-lasting medical implants
- Medicine for purposes of diagnosis, imaging and drug delivery
- Everyday items such as sunscreens, cosmetics, sporting goods and stain-resistant clothing
- Catalysis

Amongst these, the field of catalysis is the most furnished because nanocatalysts have substituted the low-quality bulk catalysts and diminish the consumption of precious noble metals with enhancement of catalytic productivity to save energy as well as time towards the green approach [13].

Nanocatalysis

Nanocatalysis is the strategic field of science since it represents a new way to meet the challenges of energy and sustainability. These challenges are becoming the main concern of the global vision of the societal challenges and world economy. Nanocatalysis became one of the most powerful tools to take on these challenges. It is also considered a part of "green science", because it often allows conducting chemical transformations in an environmentally friendly manner [14]. It plays a central role in chemical transformations and lies at the heart of countless chemical protocols, from academic research at laboratories level to the chemical industry level. It can help to design catalysts with excellent activity, selectivity as well as high stability, whose properties can easily be tuned by tailoring the size, shape and morphology of the nanocatalysts.

Common forms of nanocatalysts

- Carbon nanotubes
- Nanowires
- Nanocomposites
- Nanoporous materials
- Metal oxide nanocatalyst
- Bimetallic nanocatalyst
- Metal nanocatalysts (nanoparticles, nanoclusters etc.)

Various metals such as Ag [15-17], Au [18-20], Pt [21-23], Pd [24-29], Ni [30-32], Cu [33-35], Fe [36, 37], Ti [38], Zn [39], Rh [40-42], Ru [43-45], Ce [46] etc. based nanomaterials have been utilized as catalysts (To decrease the bulk of references, only recent selected articles are cited here).

Amongst, palladium is historically dominant over other metals, as still it is serving as a central tool for innumerable important organic transformations and total synthesis [47].

Nanocatalysts based on palladium

Downsizing of Pd based catalysts to the nanostructure is an emerging and promising field owing to the allowance of its maximum utilization, enhanced efficiency, activity and selectivity [48]. Particle size is the key function for the catalytic performance (Figure 3) wherein, on decreasing the metal size, specific activity can be increased greatly [49]. In this direction, recent advancement is going on into designing of Pd catalysts from its bulk form to nano. However, due to high surface energy and ultra-small size, Pd is very much prone to form aggregates during either synthesis or use in catalytic reactions and hence, stabilization of Pd nanocatalysts becomes necessary [50-52].

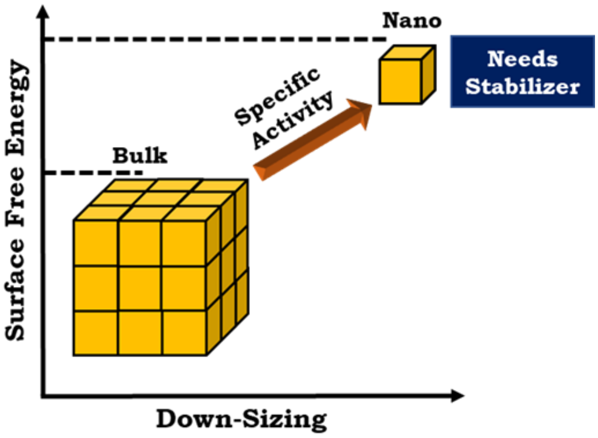

Figure 3 Miniaturization of catalyst from bulk to nano.

Generally, for nanocatalysts (NCs) two terms are associated: (i) Nanoparticles (NPs) and (ii) Nanoclusters (NCLs). The difference between NPs and NCLs lies in their sizes, NCLs are of ultra-small size (2-3 nm) [53], whereas NPs fall between 1-100 nm size. In general, we can say that all NCLs are NPs but all NPs are not NCLs. However, both NPs and NCLs are expected to show similar catalytic activity for organic transformation because of the minute nature of nano scale.

Different stabilizing agents

Stabilizer prevents the metal atoms or nanomaterials from aggregation or agglomeration during its synthesis or reaction. In this direction, number of efforts have been made to prevent the Pd nanocatalysts from the aggregation using different stabilizing scaffolds (Figure 4) [54-56], such as polymers [51, 57-70], phosphine ligands [71-74], dendrimers [75-79], surfactants [80-82], ionic liquids [83-87], heteropoly acids [13, 88-105] and others (carboxylates [106], thiols [107, 108], organic ligands [109-112] and graphite [113, 114]).

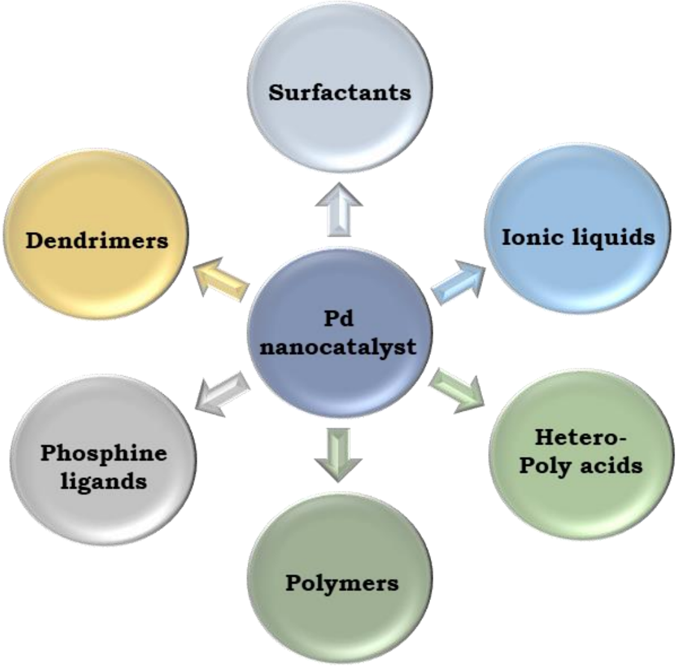

Figure 4 Different stabilizing agents.

These reported stabilizing scaffolds, except heteropoly acids (HPAs), are mostly toxic, expensive and organic and hence their use should be avoided by the replacement with some alternatives.

In this direction, **Heteropoly acids (HPAs)**, also known as polyoxometalates (POMs), are most interesting, fascinating and excellent candidates as stabilizers. They are discrete early transition metal–oxide cluster anions and comprise a class of inorganic complexes [115] having unrivalled versatility and structural variation in both symmetry and size [116].

HPAs overview

HPAs are a discrete class of anionic transition metal-oxygen clusters with unique properties of topology, size, electronic versatility as well as structural diversity ranging from nano to micrometer scale [117]. Due to these essential properties, HPAs have enjoyed a wide range of applications [118] including magnetic [119, 120], electronic and electrochemical [121-124], catalysis [125-127], optics [126, 128] and also in other fields like biology [128], nano-materials [129] and surface sciences [130].

HPAs have the general formula $[X_xM_mO_y]^{q-}$ (not as per IUPAC rule), in which X is the hetero atom, usually a main group element (e.g., P, Si, Ge and As), and M is the addenda atom, being a d-block element in high oxidation state, usually $V^{IV/V}$, Mo^{VI} or W^{VI}. These compounds are always negatively charged although the negative density is widely variable depending on the elemental composition and the molecular structure.

With the development of HPA chemistry, various types of structures were discovered [131], as listed in table 1.

Table 1 Types of HPAs

Structure	General Formula	Year of discovery
Keggin	$[XM_{12}O_{40}]^{n-}$ (X = P^{5+}, As^{5+}, Si^{4+}, Ge^{4+})	1933
Evans-Anderson	$[XM_6O_{24}]^{n-}$ (X = Te^{6+}, I^{7+})	1937
Dawson	$[X_2M_{18}O_{62}]^{n-}$ (X = P^{5+}, As^{5+})	1953
Lindqvist	$[M_6O_{19}]^{n-}$ (M = Nb^{5+}, W^{6+}, Mo^{6+})	1953
Dexter-Silverton	$[XM_{12}O_{42}]^{n-}$ (X = Ce^{4+}, Th^{4+})	1968
Keplerate	$[M_{132}O_{372}(CH_3COO)_{30}(H_2O)_{72}]^{n-}$ (M = Mo^{6+})	1998
Kortz polyoxopalladate	$[Pd_{13}As_8O_{40}H_6]^{n-}$	2008

Of all the different types of HPAs, the Keggin type HPAs are the most extensively studied because of its ease in synthesis, high thermal [6] as well as chemical stability, and the present thesis deals with Keggin type HPAs only.

Keggin type HPAs

The Keggin type HPAs have the general formula is $[XM_{12}O_{40}]^{n-}$, where X is the central hetero atom, usually a main group element like P, Si, Ge and As and M is the addenda atom, a d-block element in high oxidation state, usually V^{IV},V^{V}, Mo^{VI} or W^{VI} and formed by condensation of different mononuclear oxoanions at lower pH as shown in the following equation.

$$12MO_4^{m-} + HXO_4^{p-} + 23H^+ \rightarrow [XM_{12}O_{40}]^{n-} + 12H_2O \qquad (1)$$

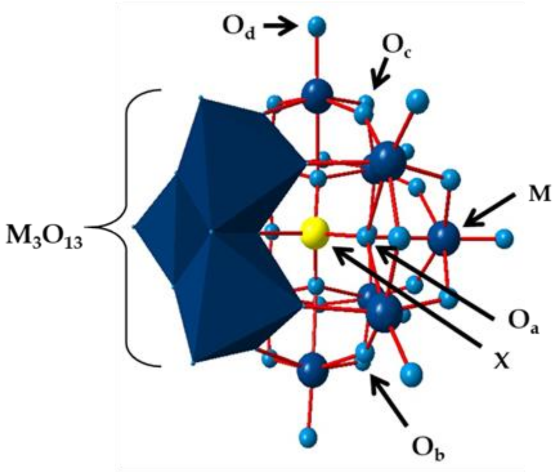

Figure 5 Structure of Keggin ion.

The ideal Keggin structure, $[XM_{12}O_{40}]^{3-}$ of α-type (Figure 5) has T*d* symmetry and consists of a central XO_4 tetrahedron (X = central heteroatom) surrounded by twelve MO_6 octahedra (M = addenda atom). The twelve MO_6 octahedra form four groups of three edge-shared octahedra, the M_3O_{13} triplet [132, 133], which have a common oxygen vertex connected to the central heteroatom. The oxygen atoms in this structure fall into four classes of symmetry-equivalent oxygens: $X\text{-}O_a\text{-}(M)_3$, $M\text{-}O_b\text{-}M$, connecting two M_3O_{13} units by corner sharing; $M\text{-}O_c\text{-}M$, connecting two M_3O_{13} units by edge sharing; and terminal $O_d\text{-}M$, where M is the addenda atom and X the heteroatom.

The advantage of HPAs as catalysts [134]

Following are the practical advantages of HPAs as catalysts.

1. **Designing at molecular level**
    - *Acidic and redox properties:* These properties of catalyst can be controlled by choosing appropriate elements (type of polyanion, heteroatom counter-cation etc.)
    - *Multifunctionality:* Acid-Redox, Acid-Base, multielectron transfer etc.
    - Tertiary structure, bulk type behavior etc. for solid state are well controlled by counter cations
2. **Molecular metal-oxide clusters**
    - Molecular designing of catalyst
    - Cluster models of mixed oxide catalyst and relationships between solution and solid catalyst
    - Description of catalytic processes at atomic/molecular level, spectroscopic study and stoichiometry are realistic
3. **Unique reaction fields**
    - *Surface type catalysis:* It is the most ordinary type of catalysis, where the reaction takes place on the surface of the solid catalyst. Here, the rate of reaction is proportional to the surface area
    - *Bulk type I catalysis:* The reactant molecules are adsorbed in the interpolyanion spaces of the ionic crystal for reaction occurans and finally, the formed products desorb from there. The classic example of this type is the acid catalyzed reaction of polar molecules over group I salts at relatively low temperature. In a sence, the solid behaves like a solution and the reaction surface becomes three-dimensional, and hence termed “pseudeliquid” catalysis. Here, the reaction rate depends on the volume of the catalyst, for instance, an acid catalyzed reaction would depend on the bulk acidity of the catalyst.

- *Bulk type II catalysis:* Although, the reaction occurs on surface, there is a rapid migration of redox carriers like electrons and protons, because of which in principle, the bulk catalyst participates in the reaction. Dehydrogenation and oxidation of hydrogen at high temperatures are classic examples of this type, and the rate of reaction is proportional to the bulk volume of the catalyst. In case of HPAs, they behave as "pseudoliquids" and hence follow bulk type II catalysis, which provide unique three-dimensional environment, and make spectroscopic and stoichiometric studies feasible and realistic

4. **Unique basicity of polyoxoanions**
    - It plays an important role in their high catalytic activity as they help in selective co-ordination as well as stabilization of reactive intermediates in solution, pseudoliquid and in solid phases

In addition they have following advantages: (i) Robust oxoanionic nature which greatly enhance the stability power [89, 93, 97, 135], (ii) reducing capacity which favors the stability of Pd into its most stable oxidation state (zero) and (iii) large relative sizes which sterically hinder PdNPs and prevent them from agglomeration during the synthesis as well as its catalytic reactions.

The road already travelled: HPA stabilized Pd- history

The first art on HPA stabilized metal nanoparticle was reported in 1952 by Chalkley, he synthesized 12-tungstophosphoric acid (α-$H_3PW_{12}O_{40}$) stabilized Ag nanoparticles by photochemical reduction of aq. $AgNO_3$ [136]. However, the first HPA stabilized Pd nanocatalyst was reported after 50 years by Papaconstantinou [88], and after that progress in HPAs stabilized Pd nanocatalysts chemistry has flourished.

In 2002, Papaconstantinou et al. reported the use of 12-tungstosilisic acid ($H_4SiW_{12}O_{40}$) as reducing as well as stabilizing agent for synthesis of Pd nanoparticles using isopropyl alcohol as sacrificial solvent. This photochemically synthesized material was characterized by TEM [88]. In the same year, Neumann et al. derived monolacunary tungstophosphate stabilized Pd nanoparticles by reduction of potassium salt of palladium substituted monolacunary tungstophosphoric acid $K_5[PPdW_{11}O_{39}]$. The synthesized material was characterized by TEM, electron diffraction measurement and ^{31}P NMR. Its catalytic efficiency was evaluated for Suzuki-Miyaura (SM), Heck, Stille-type carbon-carbon coupling and carbon-nitrogen coupling reactions of bromoarenes in aqueous media. Furthermore, they supported $K_5[PdPW_{11}O_{39}]{\cdot}12H_2O$ on γ-Al_2O_3 by impregnation method and obtained catalyst, $[K_5[PdPW_{11}O_{39}]{\cdot}12H_2O/\gamma\text{-}Al_2O_3]$ and applied the same for SM reaction using chlorobenzene as one of the substrates under solvent free condition [135].

In 2008, Liu et al. synthesized Dawson-type potassium salt of V-substituted tungstophosphate cluster ($K_9[H_4PVW_{17}O_{62}]$) and used as reducing as well as stabilizing agent for Pd nanoparticles. Synthesized material was characterized by XPS, TEM and zeta potential analysis [89].

In 2010, Corma et al. applied tetra butylmethylimidazolium molybdovanadophosphate ($[bmim]_4HPO_{40}V_2Mo_{10}$) ionic liquid for stabilization of Pd nanoparticles and characterized by elemental analysis, AAS, TGA, ^1H NMR, HAADF-STEM, HREM, XPS, XANES and EXAFS. The catalytic activity of the material was studued for Heck coupling [90].

In 2012, Yamashita et al. synthesized Pd nanoparticles stabilized via silica supported cesium salt of 12-tungstophosphoric acid ($Pd/Cs_{2.5}H_{0.5}PW_{12}O_{40}/SiO_2$) by photo-assisted deposition method and characterized by ICP, XRD, UV-vis spectroscopy, BET surface area and FT-EXAFS. It was found to be active catalyst for the direct synthesis of hydrogen peroxide [137].

In 2013, Thorimbert et al. reported the DFT study for phosphovanadotungstate polyanion $[P_2W_{15}V_3O_{62}]^{9-}$ as a powerful support to stabilize palladacycles conjugated to the inorganic framework via an organic ligand as well as its application towards Heck coupling [91]. In the same year, Kortz et al. reported the wet chemical synthetic method to prepare Pd metal nanoclusters stabilized by tetrabutylammonium salts of tungstophosphate with the well-known Keggin $[\alpha\text{-}PW_{12}O_{40}]^{3-}$, Wells–Dawson $[P_2W_{18}O_{62}]^{6-}$ and their lacunary derivatives $[\alpha\text{-}PW_{11}O_{39}]^{7-}$ and $[P_2W_{15}O_{56}]^{12-}$ structures. These stabilized catalysts were characterized by EDX, TEM, UV-vis spectroscopy, FT-IR, XRD and XPS. The activity of the synthesized materials was evaluated for 1-hexene hydrogenation and comparison showed the exceeding activity of $[P_2W_{18}O_{62}]^{6-}$ stabilized Pd nanoclusters compared to all others [92]. They have also reported the use of novel Krebs type tetrabutylammonium salt of various polyoxoanions $[(TBA)_4H_4[M_4(H_2O)_{10}(XW_9O_{33})_2]$, where M = Mn, Ni, Zn, X = Te, Se; M = Fe, X = Sb, As] as stabilizers for Pd(0) metal clusters and characterized them by EDX, TEM, UV-vis spectroscopy, FT-IR, XRD, and XPS. Catalytic activity of the designed materials was assessed for hydrogenation of cyclohexene and 1-hexene [93], in the same year. Simultaneously, Yuan et al. reported a novel method for the synthesis of bimetallic Pt and Pd nanoparticles deposited on multiwalled carbon nanotubes (MWCNTs) using 12-molybdophosphoric acid ($H_3PMo_{12}O_{40}$) as stabilizer. This $H_3PMo_{12}O_{40}$/PtPd/MWCNT nanotubes was characterized by FT-IR, XPS, TEM, ICP-AES and explored as electrocatalysts for the methanol electrooxidation [94].

In 2014, Cronin et al. developed one-pot strategy for the synthesis of stabilized palladium via potassium salt of selenotungstic acid isomers $K_{28}[H_{12}Pd_{10}Se_{10}W_{52}O_{206}]\cdot 65H_2O$ and $K_{26}[H_{14}Pd_{10}Se_{10}W_{52}O_{206}]\cdot 68H_2O$ as well as sodium salt of tellurotungstic acid cluster $Na_{40}[Pd_6Te_{19}W_{42}O_{190}]\cdot 76H_2O$ [95] and characterized by SCXRD. In the same year, Proust et al. also invented simple procedure for vacant tungstophosphates ($[PW_{11}O_{39}]^{7-}$ and $[P_2W_{19}O_{69}(H_2O)]^{14-}$) and tungstoarsenate ($[As_2W_{19}O_{67}(H_2O)]^{12-}$) stabilized palladium (0) nanoparticles in water by hydrogenation with H_2 at ambient temperature and atmospheric pressure. [97]. These crystalline materials were characterized by EDX, SCXRD, FT-IR, Raman, ^{31}P NMR, TEM, HRTEM and XPS.

In 2015, Han et al. reported one-pot synthesis for 12-tungstophosphoric acid stabilized Pd nanocrystals ($H_3PW_{12}O_{40}$ Pd NCs). This stabilized NCs was characterized by SEM-EDX, TEM, UV-vis spectroscopy, FT-IR, ICP, CV and XPS. The material was utilized for chemical (Suzuki coupling) and electrochemical catalysis (formic acid oxidation) [96]. In the same year, Ahmadpour et al. demonstrated the use of 12-molybophosphoric acid as stabilizing agent for Pd nanoparticles supported on graphene nanosheets ($Pd/H_3PMo_{12}O_{40}/GNSs$). The synthesized material was characterized by EDX, SEM, TEM, HAADF-STEM, XRD and proved its synergistic behavior for enhanced ethanol electrooxidation reaction and shows better tolerance to poisoning species [13]. During the same period, Wei et al. prepared 12-molybdophosphoric acid stabilized supported palladium nanoparticles ($Pd/PMo_{12}O_{40}$) by *in situ* reduction method and characterized by BET surface area, XRD, SEM, TEM, HRTEM and XPS. Moreover, they proved it as a superior nanocatalyst to carbon supported platinum for promotion of the oxygen reduction reaction, i.e. serves as an assistant catalyst, facilitating the decomposition of the harmful hydrogen peroxide intermediates [98].

In 2016, Chen et al. designed one pot- method for tetra metal substituted sandwich phosphorotungstate $[M_4(H_2O)_2(PW_9O_{34})_2]^{10-}$ (where, M = Fe^{2+}, Co^{2+}, Mn^{2+}, Cu^{2+} and VO^{2+}) stabilized Pd nanoparticles, encapsulated *in situ* in mesoporous aluminum phosphate (mAPO). Synthesized material was characterized by XRD, TEM, BET surface area, ICP, FT-IR, UV-vis spectroscopy and their catalytic efficiency were evaluated towards aerobic oxidation of alcohol in water [99]. Simultaneously, Zhang et al. developed facile and green one-pot synthetic method for 12-tungstophosphoric acid stabilized tri-component catalyst comprising of Pd nanoparticles on macroporous carbon ($Pd@\ H_3PMo_{12}O_{40}/MPC$) and characterized by XRD, SEM, TEM, EDX, XPS and CV. The synthesized catalyst was to promote the development of new electrochemical sensors and electrode materials [100]. In the same year, Han et al. reported one-pot synthesis for 12-molybdophosphoric acid stabilized bimetallic Pt and Pd based core-shell nanocrystals (Pd/Pt@$H_3PMo_{12}O_{40}$) and characterized by SEM, TEM, HAADF-STEM, EDX, ICP-AES, XPS and XRD. The efficiency of the material was evaluated for electrooxidation of methanol [101].

In 2017, Zhao et al. fabricated 12-tungstophosphoric acid stabilized palladium nanoparticles on reduced graphene oxide (Pd/$H_3PW_{12}O_{40}$/RGO) by a simple one-pot photoreduction method and characterized by TEM, EDX, XRD, XPS and ICP. The synthesized catalyst was used for electrooxidation of ethylene glycol and glycerol [102]. Parallelly, Zhang et al. designed ex-situ decorated ordered mesoporous carbon with palladium nanoparticles via 12-tungstophosphoric acid stabilization (Pd-$H_3PW_{12}O_{40}$-OMC) and characterized by SEM, TEM, EDX, BET surface area, XRD and XPS. The efficiency of this tri-component system was evaluated for sensitive detection of acetaminophen in pharmaceutical products [103].

In 2018, Leng and Dai anchored palladium nanoparticles on a 12-tungstophosphoric acid attached to melem ($C_6H_6N_{10}$; 2,5,8-triamino-heptazine) porous hybrid ($H_3PW_{12}O_{40}$/melem, as stabilizing agent) by hybridization and post chemical reduction, and characterized by FT-IR, SEM, ICP-AES, UV-vis spectroscopy, TEM, HRTEM, H_2-TPR, XRD and XPS. The efficiency of the catalyst was studied towards formic acid dehydrogenation [104]. In this catalytic system, melem plays an important role for hydrogen transfer and accelerate the hydrogen generation. At the same time, Zhang et al. developed tricomponent stabilized nanohybrid comprising of Pd, 12-tungstophosphoric acid and nitrogen-doped hollow carbon spheres (Pd/$H_3PW_{12}O_{40}$/NHCS). Synthesized nanohybrid material was characterized by XRD, SEM, TEM and XPS, and assessed its activity as selective electrochemical sensor for acetaminophen [105].

A literature survey shows that different HPAs have been used as stabilizing agents. ***In the present case, we have selected 12-tungstophosphoric acid (TPA) as a stabilizing agent because of its following properties.***

- Most acidic
- Thermally most stable
- Multifunctional
- Encapsulating agent
- Reducing agent
- Exchangeable protons

Stabilized NCs can be divided into mainly three types:

1. Homogeneous NCs

The main advantage of homogeneous catalysis is that the catalyst mixes into reaction mixture, allowing a very high degree of interaction between catalyst and reactant molecules to enhance the rate of product formation. Traditionally almost all chemical reactions were catalyzed by homogeneous catalysts. However, it depends on the applications, such as, for the production of bulk chemicals (e.g. NH_3; H_2SO_4), the catalysts are often heterogeneous. The enforcement of stringent environmental regulations has forced the replacement of the homogeneous catalysts by alternative one due to the following associated disadvantages.

- High solubility
- Low thermal stability
- Tedious recovery process from the reaction mixture
- Reusability

The aforementioned disadvantages of homogeneous catalysts can be overcome by immobilization of NCs into liquid phases or by supporting/anchoring NCs onto suitable solid support (heterogenization).

2. *Immobilized NCs into liquid phases/onto supported ionic liquid phase (SILP)/onto supported aqueous phase (SAP)*

For the immobilization of NCs, different solvents such as water [138], ionic liquids [139], $scCO_2$ [140], polyols [141, 142] etc. are commonly used. Usually, these greener solvents, in contrast to volatile organic compounds, can play several roles, such as stabilizer, reductant, and/or liquid phase for trapping nanocatalysts, thus facilitating their recycling. However, in some cases there is a need of some external stabilizing agent (especially in case of lower polyols) [56]. NCs can also be immobilized onto supported ionic liquid phase (SILP) as well as supported aqueous phase (SAP) [143].

3. *Supported/anchored NCs onto suitable solid supports (Heterogeneous)*

Supports provide large surface area for the dispersion of NCs. The catalyst molecule gets dispersed onto the surface of support or inside the pores of support and thus available for the combination with reactant as in homogenous catalyst. The resulting heterogeneous catalyst can function mechanically as if it was in solution but it would operate as a separate immobile phase and thus, the advantages of both homogenous and heterogeneous catalysts are retained.

Most important advantages of heterogeneous catalysts from the view point of chemical reaction systems are:

- High surface area
- Enhanced thermal and chemical stability
- High catalytic activity and selectivity
- Ease of separation from reaction mixture
- Regeneration and Recycling
- Process simplification under mild and sustainable reaction conditions
- Can be ‘tailored’ for specific feedstock or for selective product synthesis
- Kinetically and thermodynamically difficult reactions can proceed with wide range of temperature, even in gas phase

However, the main disadvantage of heterogeneous catalysis is leaching of the active species from the support.

In the present study, our main focus is the supporting/anchoring of PdNCs onto the suitable support and to overcome the leaching of active species.

For metal-based catalysts the given definitions of homogeneous and heterogeneous catalysis are not strictly precise. Another perspective was given by Schwartz, the reaction in which the substrate molecules encounter a single type of active metal sites (in some cases two) termed as homogeneous catalysis whereas, encounter toward multiple active sites referred as heterogeneous catalysis [144].

Different methods of supporting

One of the important steps in designing a nanocatalyst is supporting of active species onto the support. Either the support can be in a preformed state or both can be formed together from the solution simultaneously.

Commonly used methods for supporting are as follow.

1. Co-precipitation
2. Deposition precipitation
3. Dry impregnation/incipient wet impregnation
4. Equilibrium adsorption/ion exchange

As impregnation, is one of the most accepted method for preparation of supported catalysts, we are focusing on this method only.

Impregnation [145]

Impregnation is a preparation technique in which a solution of the precursor of the active phase is brought in contact with the support. Two methodologies exist. (i) Dry impregnation: Also referred to as “pore volume impregnation”, just enough liquid (solution of the precursor) is used to fill the pore volume of the support. (ii) Incipient wet impregnation: The support is dipped into an excess quantity of solution containing the precursor of the active phase.

In dry impregnation, the solubility of the catalyst precursors and the pore volume of the support determine the maximum loading available each time of impregnation. If a high loading is needed, successive impregnation (and heat treatment) may be necessary. In the first step of impregnation, three processes occur:

- Transport of solute to the pore system of the support bodies
- Diffusion of solute within the pore system
- Uptake of solute by the pore wall

In the case of wet impregnation, a fourth process is operative, *viz.* transport of solute to the outer particle surface. Depending on the process conditions, different profiles of the active phase over the transport body will be obtained.

Choice of the support

The choice of support is a crucial step in heterogeneous nanocatalysis. The most important is stability. The support must be stable up to high temperature, under reaction condition and regeneration conditions. It should be inert with solvent, reactants or reaction products. A support must be easily available, either commercially or should be easily synthesized.

Dispersion of active species on supports with high surface areas is important for catalytic application. In general, HPAs strongly interact with supports at low loading levels, while the bulk properties of HPAs prevail at high loading levels. Nature of the support also plays a crucial role in determining the activity of catalyst. It was found that acidic or neutral supports are suitable to enhance catalytic activity of HPAs. In addition, basic support cannot be used for anchoring HPAs, since it gets decomposed in the basic environment. As mentioned, when acidic supports are used, strong interaction is expected between non-bonding oxygens of HPAs and protons from -OH groups of the supports.

A literature survey also shows that number of reports are available on catalytic aspects of HPA stabilized Pd nanocatalyst supported on to different supports, such as alumina [135], silica [137], carbon [100, 103, 146], carbon nanotube [94], graphene nanosheets [13], reduced graphene oxide [102], aluminum phosphate [48], melem porous hybrid [104] and polymer [147].

In the present work, hydrous zirconia (ZrO_2, an acidic support) was selected as support due to the following reasons:

- Physical properties can easily be modified by surface treatment
- Mechanical properties similar to those of stainless steel
- Thermodynamically stable modification up to a temperature of 2370°C [148, 149]
- Direct anchoring surface which facilitates the easy approach of substrates to active sites via available surface hydroxyl groups for the interaction
- Our expertise in the field of ZrO_2 supported catalytic systems

❖ ***To see the effect of support, another acidic metal oxide support, silica (SiO_2) was selected***

C-C coupling and hydrogenation have been selected for evaluation of catalytic activity as still both are important and fascinating in industries as well as in academia. Bearing in mind the importance of the said reactions and environmental point of view, C-C coupling (SM and Heck) and hydrogenation reactions are selected as model reactions for the catalytic evaluation of the designed nanocatalysts. Both the reactions were carried out in aqueous medium as well as in neat water.

C-C cross coupling reactions

C-C cross-coupling reactions in organic chemistry are a general term for a variety of reactions where two fragments nucleophile and electrophile are bonded together by the means of C-C bond, predominantly Pd mediated. They are extensively used in the synthesis of number of industrially important organic compounds [150, 151]. It wouldn't have been possible to synthesize some of the complex natural products or synthetic compounds (Figure 6) without using C-C coupling in one or more steps [152, 153].

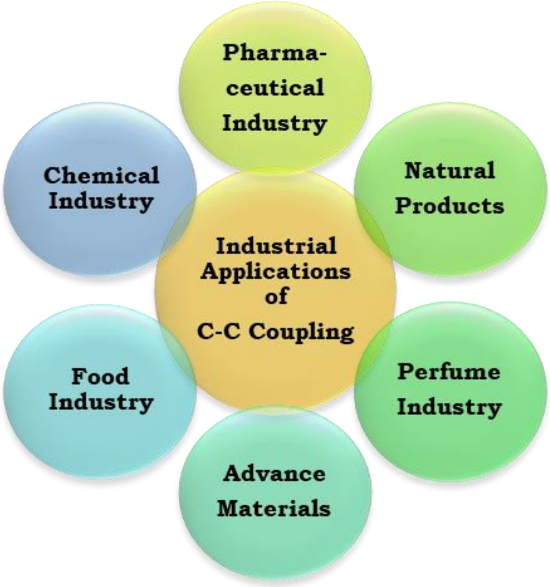

Figure 6 Industrial applications of C-C coupling reactions.

Different types of C-C coupling

Literature shows that there are various types of C-C coupling reactions available in arts and few of them are: Suzuki-Miyaura (SM), Heck, Sonogashira, Stille, Negishi, Kumada, Hiyama etc. The following chart (Figure 7) shows the research popularity on these C-C coupling reactions since 1990 onwards to till date (data collected from Sci-Finder). Which clearly depicts substantial growth in this area has taken place during the last three decades in terms of publications with the SM cross-coupling proving by far the most popular, followed by the Heck that SM and Heck coupling reactions are the most researched amongst all.

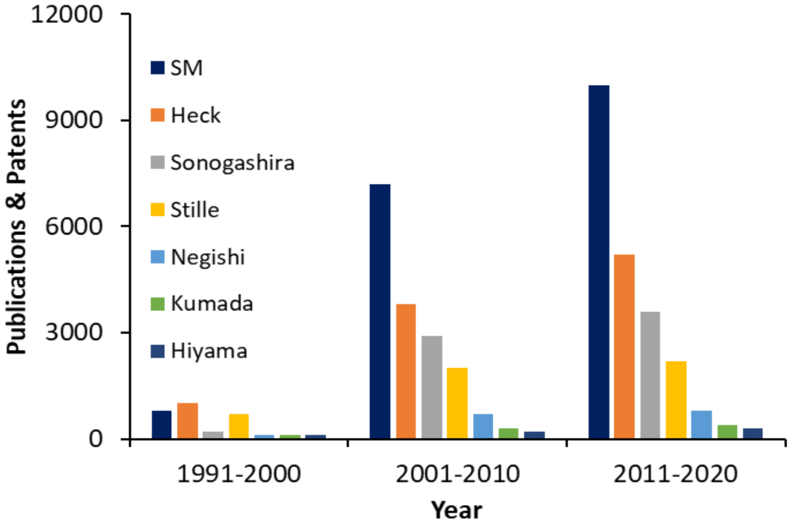

Figure 7 Research popularity on cross coupling reactions.

Invention of cross couplings between carbon atoms, using palladium as a catalyst by Prof. Richard Heck (Heck coupling), Prof. Ei-ichi Negishi (Negishi coupling) and Prof. Akira Suzuki (SM coupling) have gained noble recognition (Figure 8). These reactions are highly relevant even today, after more than 4 decades of the discovery using Pd, which reflects in terms of huge number of publications every year.

However, we have restricted ourselves for the literature related to the stabilized palladium nanocatalysts by HPAs only.

Prof. Richard Heck
Photo source:
https://www.nobelprize.org/prizes/chemistry/2010/heck/biographical/
First developed - 1969

Prof. Ei-ichi Negishi
Photo source:
http://www.washington.edu/news/2011/02/23/20
First developed - 1976

Prof. Akira Suzuki
Photo source:
https://www.mcgill.ca/science/20140318-public-lecture-akira-suzuki
First developed - 1979

Figure 8 Noble laureates for Heck, Negishi and SM coupling inventions.

Hydrogenation

Hydrogenation is still one of the most important reactions in organic chemistry. It is a chemical reaction between molecular hydrogen and unsaturated compound, usually performed in presence of a catalyst such as nickel, palladium or platinum. The process is commonly employed to reduce or saturate organic compounds. The earliest hydrogenation was carried out for addition of hydrogen to oxygen using platinum as catalyst in the Döbereiner's lamp, which was commercialized in 1823 as device. In 1897, French chemist, Paul Sabatier had invented the process of nickel catalyzed hydrogen addition to the gaseous hydrocarbons. For this discovery, he is considered as father of the hydrogenation process and gained noble recognition in 1912.

C-C cross coupling

- ***Suzuki-Miyaura (SM) coupling***

SM coupling is extremely powerful tool for the formation of C-C bonds, displaying a number of advantageous features: (i) Easily handled and usually air and moisture stable organoboron starting materials; (ii) Mild and convenient reaction conditions and (iii) The facile removal of less-toxic inorganic by-products. These aspects make it useful especially for industrial applications.

In literature only two reports are found on SM coupling by TPA stabilized Pd nanocatalysts. First in 2002, Neumann et al. derived palladium nanoparticles from a palladium substituted mono lacunary tungstophosphoric acid ($K_5[PPdW_{11}O_{39}]\cdot 12H_2O$) and utilized for SM coupling. They used 1 mol% Pd, diisopropylamine as base, (2:8) mL ethanol-water mixture as solvent to achieve 94 % yield of biphenyl at 85 °C in 12 h using bromobenzene as coupling substrate. Further, they supported $K_5[PdPW_{11}O_{39}]\cdot 12H_2O$ on γ-Al_2O_3, used as a heterogeneous catalyst for base/solvent free SM coupling of cholorobenzene and obtaind 99 % yield of biphenyl with 1.17 mol% Pd at 130 °C in 16 h [135].

Secondly in 2015, Han et al. reported one-pot synthesis of 12-tungstophosphoric acid stabilized Pd nanocrystals ($H_3PW_{12}O_{40}$ Pd NCs). The resultant Pd nanocatalyst was applied for the SM coupling using, 0.1 mol% Pd, K_3PO_4 base and (4:1 mL) ethanol-water mixture to obtain 92 % yield at 60 °C in 3 h [96].

- ***Heck coupling***

The independent and almost concurrent discoveries by Mizoroki [154, 155] and Heck [156, 157] demonstrated the coupling reactions of aryl, benzyl, and styryl halides with alkenes employing palladium catalysts, and set the stage for the evolution of the Mizoroki-Heck reaction (hereafter, as "Heck" reaction).

In-spite of having numerous advantages only one report is available in art, on Heck coupling over TPA stabilized PdNCs, by Neumann et al. in 2002. As discussed in SM coupling, the synthesized catalyst $K_5[PdPW_{11}O_{39}]{\cdot}12H_2O$ was used for Heck coupling of *p*-bromotoluene using 1 mol% Pd, diisopropylamine as base and (2:8 mL) ethanol-water mixture at 85 °C, 16 h to achieve 95 % yield of stilbene derivative [135].

Hydrogenation

In literature, only two reports were found on hydrogenation, catalyzed by TPA stabilized Pd nanocatalyst by Kortz et al. First in 2013, they reported Pd nanoclusters stabilized by tetrabutylammonium salts of tungstophosphates with the well-known Keggin $[\alpha\text{-}PW_{12}O_{40}]^{3-}$, Wells–Dawson $[P_2W_{18}O_{62}]^{6-}$ and their lacunary derivatives $[\alpha\text{-}PW_{11}O_{39}]^{7-}$ and $[P_2W_{15}O_{56}]^{12-}$ structures. The activity of the synthesized materials was evaluated for 1-hexene hydrogenation and comparison showed the exceeding activity of $[P_2W_{18}O_{62}]^{6-}$stabilized Pd nanoclusters compared to all (100 % conversion under 5 bar H_2 pressure, 4.17 mol% Pd, 30 °C in 20 min) [92]. Second, in the same year, they reported the use of novel Krebs type tetrabutylammonium salt of various polyoxoanions $[(TBA)_4H_4[M_4(H_2O)_{10}(XW_9O_{33})_2]$, where M = Mn, Ni, Zn, X = Te, Se; M = Fe, X =

Sb, As] as stabilizers for Pd(0) metal clusters. The catalytic activity of the designed materials was assessed for hydrogenation of cyclohexene and 1-hexene at 30 °C under 5 bar continuous H_2 pressure using 0.36 mol% Pd [93].

A literature survey shows that:

- Despite distinct advantages of TPA stabilized Pd nanocatalysts such as enhanced activity, selectivity and non-toxic nature, reports on their synthesis, characterization as well as catalytic activity are very scarce
- The use of such catalysts for C-C couplings (SM and Heck) as well as hydrogenation is restricted to five reports only
- Further designing of zirconia supported TPA stabilized Pd nanocatalysts are not available in the art
- The use of water as green solvent for hydrogenation is untouched

Based on these observations, the objectives of the thesis have been proposed.

Objectives of the Thesis

- To synthesize Palladium nanocatalysts (PdNCs) stabilized by Zirconia supported TPA/LTPA (12-tungstophosphoric acid/mono lacunary tungstophosphoric acid) using ion exchange method.
- To design stabilized Palladium nanocatalyts (PdNCs) based on TPA/LTPA using salt method
- To convert above synthesized homogeneous nanocatalysts into heterogeneous by supporting/anchoring onto ZrO_2/SiO_2.
- To characterize all synthesized nanocatalysts by various techniques such as EDX, FT-IR, TGA, ^{31}P MAS NMR, XPS, Powder XRD, BET Surface Area, SEM, TEM, HRTEM and STEM
- To use the synthesized catalysts for C-C coupling (Suzuki-Miyaura and Heck) and hydrogenation under mild conditions (aqueous medium and neat water)
- To study different reaction parameters such as substrate to catalyst ratio, temperature, pressure, time and solvent for maximum conversion as well as product selectivity
- To overcome the leaching of active species from the support
- To study the sustainability of the catalysts by multiple regeneration and characterization
- To study reaction mechanism
- To compare the efficiency of all the catalysts and to propose the best method of designing as well as catalyst for the said reactions

Organization of the thesis

The work has been divided into two parts consisting five chapters and an annexure:

Part A: Ion Exchange Method

Chapter 1	**PdNPs Stabilized by Zirconia Supported TPA: Synthesis, Characterization and Applications to C-C coupling and Hydrogenation**
Chapter 2	**PdNPs Stabilized by Zirconia Supported LTPA: Synthesis, Characterization and Applications to C-C coupling and Hydrogenation**

Part B: Salt Method

Chapter 1	**Stabilized PdNCLs by TPA: Synthesis, Characterization and Applications to C-C coupling and Hydrogenation**
Chapter 2	**Zirconia Supported Stabilized PdNCLs by TPA: Synthesis, Characterization and Applications to C-C coupling and Hydrogenation**
Chapter 3	**Zirconia Supported Stabilized PdNCLs by LTPA: Synthesis, Characterization and Applications to C-C coupling and Hydrogenation**
Annexure	**Silica Encapsulated Stabilized PdNCLs by TPA: Synthesis, Characterization and Applications to C-C coupling and Hydrogenation**

Brief discussion of each chapter

Part A: Ion Exchange Method

Chapter 1 describes the synthesis of PdNPs stabilized by Zirconia supported TPA. The synthesized catalyst is characterized by various instrumental techniques such as EDX, TGA, FT-IR, XPS, TEM, HRTEM, HAADF-STEM, BET and powder XRD. The activity of the catalyst is studied for SM and Heck coupling (in aqueous medium and water) as well as hydrogenation in water by varying different reaction parameters. Leaching and heterogeneity tests are performed for the sustainability evaluation of the catalyst. Used catalyst is recovered and regenerated to probe its activity for number of catalytic runs. Regenerated catalyst is characterized by EDX, XRD, BET and XPS in order to check its stability. Viability of the catalyst towards different substrates as well as activity comparison with reported systems are discussed. Further, detail mechanistic investigation for crotonaldehyde hydrogenation is also carried out.

Chapter 2 deals with the synthesis and characterization of PdNPs stabilized by Zirconia supported LTPA. The activity of the catalyst is studied for SM and Heck coupling in aqueous medium as well as hydrogenation in water by varying different reaction parameters. Control experiments, leaching and heterogeneity tests are performed. Spent catalyst is recovered and regenerated to probe its activity for five catalytic runs. Regenerated catalyst is characterized in order to check its stability. Scope of the catalysis, activity of the catalyst with reported systems as well as the effect of addenda atom on the reactions are also evaluated.

Part B: Salt Method

Chapter 1 describes the synthesis of stabilized PdNCLs by TPA, followed by detail characterization by various physico-chemical techniques. The efficiency of the catalyst is evaluated towards SM and Heck coupling in aqueous medium as well as hydrogenation in water.

Chapter 2 describes the synthesis and characterization of Zirconia supported stabilized PdNCLs by TPA. The activity of the catalyst is evaluated for SM and Heck coupling in aqueous medium as well as hydrogenation in water by varying different reaction parameters. To investigate the role of each component, control experiments are carried out under optimized reaction conditions. Leaching and heterogeneity tests are performed for the sustainability evaluation of the catalyst. Recycling study is performed up to five cycles and regenerated catalyst is characterized by EDX, FT-IR, XRD, BET, and XPS in order to check its stability. Scope of the substrates is studied for different functionalities. Activity of the catalyst is also compared with the reported systems.

Chapter 3 deals with the synthesis of stabilized PdNCLs by LTPA as well as its supporting onto Zirconia followed by its detail characterization. The activity of the catalyst is studied for SM and Heck coupling in aqueous medium as well as hydrogenation in water by varying different reaction parameters. Control experiments, leaching and heterogeneity tests are carried out. Regeneration study of the catalyst as well as characterization of regenerated catalyst are performed. Tolerance limit of the catalyst is investigated for variety of the substrates. Activity of the catalyst with reported systems as well as the effect of addenda atom on the reactions are also evaluated.

The comparison of activity of all the synthesized catalysts is investigated and discussed on the bases of acidity as well as counter protons.

Annexure depicts the synthesis and characterization of silica encapsulated stabilized PdNCLs by TPA. The activity of the catalyst is studied for SM and Heck coupling in aqueous medium as well as hydrogenation in water by varying different reactions parameters. Leaching and heterogeneity tests are performed for the sustainability evaluation of the catalyst. Used catalyst is recovered and regenerated to probe its activity for five catalytic runs. Scope of the substrates is carried out for different functionalities. Regenerated catalyst is characterized in order to check its stability. The detailed mechanistic investigation for cyclohexene hydrogenation is also carried out.

At the end of thesis, the effect of supports (ZrO_2 and SiO_2) on the activity of the catalysts has also been compared and discussed.

Analytical techniques utilized in the present work

A prime aspect in a nanocatalyst development is the characterization [158-160]. In general, and especially in supported nanocatalysts, the elucidation of the structures, composition as well as chemical properties of the synthesized materials and the interactions between active species as well as the supports is essential to understand the relationship between the catalytic properties of the material and its catalytic performance [160]. It is also crucial to know the basis of the structure-catalytic properties of the materials to further synthesize new catalysts.

In case of supported catalysts, it is crucial to know if the active ingredient is on the surface of the support or diffuse in it. As a result, from the scientific point of view, the investigation of the surface composition as well as local structure of catalyst at the atomic level and the correlation of these data with catalyst performance is very important in the catalytic reaction. The basic information on the structure-catalytic property relationship for catalytic systems will ultimately be of value in the design of new efficient catalysts. Heterogeneous catalyst can be characterized by various tools which comprise different physicochemical and spectroscopic techniques. A brief introduction of the various characterization techniques for nanocatalysts that have been used for the present study is shown below:

Energy-dispersive X-ray spectroscopy (EDS or EDX) [161]

EDS or EDX is an analytical technique used for the elemental analysis or chemical characterization of a sample. It relies on the investigation of a sample through interactions between electromagnetic radiation and matter, analyzing

X-rays emitted by the matter in response to being hit with charged particles. Its characterization capabilities are due in large part to the fundamental principle that each element has a unique atomic structure allowing X-rays that are characteristic of an element's atomic structure to be identified uniquely from one another.

The elemental analysis was carried out using JSM 5610 LV combined with INCA instrument for EDX-SEM analyzer for the quantitative identification of metal ions.

Thermo Gravimetric Analysis (TGA) [162]

It is a technique whereby the weight of a substance, in an environment heated or cooled at a controlled rate, is recorded as a function of time or temperature.

The temperature-weight loss profile of a supported catalyst can provide important quantitative information on the types of water present in the sample. It is usually possible to distinguish loosely held “physisorbed” water from strongly bonded “chemisorbed” water and helps determine the best conditions for removing the former.

More usefully, the study of the decomposition of less stable catalysts can also be done which help in determine the maximum activation temperatures and the temperatures at which the supported reagents can be safely used in reactions.

TGA measurements were carried out on the Mettler Toledo Star SW 7.01 in the temperature range 40 °C to 600 °C. All measurements were carried out under nitrogen atmosphere with a flow rate of 2 mL/min and a heating rate of 10 °C/ min.

Fourier Transform Infrared Spectroscopy (FT-IR) [161]

FT-IR spectroscopy is probably the most useful and widely used technique to study supported reagents. It provides the following information.

1. Identification of the surface species
2. Dispersion of the reagent over the support surface
3. Surface activity studies with the use of probe molecules

The most common ways of studying an insoluble solid are: 1) as a mull; 2) as a disc; and 3) directly as a powder. These methods differ in terms of degree of difficulty (in obtaining useful spectra), ease of sample preparation, and reliability of the information obtained. Both the mull and disc methods are transmittance techniques. FT-IR opaque or highly scattering materials may not be suitable for analysis by transmission spectroscopy.

FT-IR absorption spectra of various catalysts were recorded on a FT-IR Shimadzu (IR Affinity 1S) instrument at room temperature using KBr pellets in the range of 4000 cm^{-1} to 400 cm^{-1}. The powdered samples were ground with KBr in 1: 10 ratio and pressed (5 ton/cm^2) for making the pellets. The data were collected at an average of 40 scans.

Solid state MAS Nuclear Magnetic Resonance (NMR) Spectroscopy [163]

In nuclear magnetic resonance, Magic Angle Spinning (MAS) is a technique often used to perform experiments in solid-state NMR spectroscopy.

By spinning the sample (usually at a frequency of 1 to 70 kHz) at the magic angle θ_m (ca. 54.74°, where $\cos^2 \theta_m = 1/3$) with respect to the direction of the magnetic field, the normally broad lines become narrower, increasing the resolution for better identification and analysis of the spectrum.

NMR is an important tool to understand the environment around a particular nucleus of the synthesized material. Further, it also helps to know whether the synthesized material is pure or shows presence of isomers.

Solid state ^{31}P MAS NMR was carried out by using JOEL ECX 400 MHz High Resolution Multinuclear FT-NMR spectrometer for solids.

Powder X-Ray Diffraction (XRD) [161]

XRD can be used to detect poorly dispersed or macro-crystalline reagent. In principle, XRD can be used to give quick information on the efficiency of dispersion of any supported reagent where the reagent normally exists in the crystalline state. XRD may also be useful for the identification of species formed during the preparation on subsequent chemistry of a supported reagent. This can be especially useful for unstable reagents, corrosive reagents and where the supported reagent has been subject to high-temperature thermal treatment. XRD has also been used to characterize the nature of surface species.

The powder X Ray Diffraction pattern of support and the catalysts was obtained by using the instrument Philips Diffractometer (Model PW - 1830). The conditions used were Cu Kα radiation (1.5417 Å), scanning angle from 10° to 80°.

BET Measurement [162]

As surface area of the catalyst is directly proportional to the catalytic activity of the heterogeneous catalysts, the measurement of the surface area is most important study for the same. Further from the surface area, one can get the information on the pore volume, pore size which will be helpful to understand the mechanism of the reaction occurs.

Surface area and pore size distribution of various catalysts were measured according to Brunauer-Emmett-Teller (BET) method, involving nitrogen adsorption-desorption using Micromeritics Surface area Analyzer (Model: ASAP 2020) at -196 °C. From the adsorption desorption isotherms specific surface area was calculated using BET method. The samples were degassed under vacuum (5 – 10.3 mmHg) between 60 - 90 °C for 4 h, prior to measurement, to evacuate the physisorbed moisture. Further, the pore size distributions were calculated applying the Barrett-Joyner-Halenda (BJH) method to the desorption branches of the isotherm.

X-ray photoelectron spectroscopy (XPS) [164]

XPS is a surface-sensitive quantitative spectroscopic technique that measures the elemental composition at the parts per thousand range and electronic state of the elements that exist within a material. XPS spectra are obtained by irradiating a material with a beam of X-rays while simultaneously measuring the kinetic energy and number of electrons that escape from the top 0 to 10 nm of the material being analyzed under high vacuum ($P \sim 10^{-8}$ millibar) or ultra-high vacuum (UHV; $P < 10^{-9}$ millibar) conditions.

XPS measurements were performed with Auger Electron Spectroscopy (AES) Module PHI 5000 Versa Prob II.

Transmission Electron Microscopy (TEM) [162], High-Resolution Transmission Electron Microscopy (HRTEM) [165] and Scanning Transmittance Electron Microscopy (STEM) [166]

TEM and HRTEM (an imaging mode of specialized TEM) is a technique that uses an electron beam to image a nanoparticle sample, providing much higher resolution than is possible with light-based imaging techniques. The images can be resolved over a fluorescent screen or a photographic film. Furthermore, the analysis of the X-ray produced by the interaction between the accelerated electrons with the sample allows determining the elemental composition of the sample with high spatial resolution. TEM is the preferred method to directly measure nanoparticle size, grain size, size distribution, and morphology.

STEM images are a type of TEM images which are formed by focusing electron beam to a fine spot (with the typical spot size 0.05 – 0.2 nm) passing through a sufficiently thin specimen which is then scanned over the sample in a raster illumination system constructed so that the sample is illuminated at each point with the beam parallel to the optical axis. STEM imaging is used to characterize the nanoscale, and atomic scale structure of specimens, providing important insights into the properties and behavior of materials.

TEM micrographs were recorded on TEM CM 200 (Make: PHILIPS, Model: CM 200, Specification: Operating voltages: 20-200kv and Resolution: 2.4 Å). HRTEM analysis were carried out on Field Emission Gun-Transmission Electron Microscope (Resolution: Point: 0.19 nm, Line: 0.1 nm, Magnification: 50 x - 1.5 M x accelerating voltage of 200 kV; Make: JEOL; Model: JEM 2100F) with attachment systems EDS and STEM. The samples were dispersed in ethanol and ultrasonicated for 5–10 min. A small drop of the sample was then taken on a carbon coated copper grid and dried before viewing.

Acidity measurement

The acidity of the catalyst measured by this technique allows us to evaluate the total number of acid sites as well as their acidic strength. In order to interpret the results, it is suggested that the initial electrode potential (Ei) indicates the maximum acid strength of the surface sites and the range where the plateau is reached (meq/g solid) indicates the total number of acid sites [167], [168].

A small quantity (0.1 mL) of 0.05 N, n-butylamine in acetonitrile was added to a suspension of 0.5 g of the catalyst in 50 mL of acetonitrile and the system was stirred at 25 °C. Then, the suspension was potentiometrically titrated against 0.05 N, n-butylamine in acetonitrile. The electrode potential variation was measured with a digital pH meter.

Acidity measurement of all the synthesized nanocatalysts is carried out for overall comparison of catalytic activity, only.

Gas Chromatography (GC) [169]

GC is a type of chromatography used to separate and analyze the material, which vaporized without decomposition. Its main applications include testing purity of a compound and separation of components of a mixture. In the present work, all the GC experiments were carried out on Shimadzu GC-2014 instrument using Rtx-5 capillary column and flame ionization detector (FID).

References

[1] R. P. Feynman, California Institute of Technology, Engineering and Science magazine, (1960).

[2] M. Faraday, The Bakerian Lecture. —Experimental relations of gold (and other metals) to light, Phil. Trans. R. Soc., 147, 145-181, (1857).

[3] N. Taniguchi, On the Basic Concept of Nanotechnology. Proceedings of the International Conference on Production Engineering, Tokyo, 18-23, (1974).

[4] K. E. Drexler, Proc. Natl. Acad. Sci., 78, 5275-5278, (1981).

[5] K. E. Drexler, Engines of creation, Anchor, (1986).

[6] A. Javey, ACS Nano, 2, 1329-1335, (2008).

[7] M. G. Bawendi, P. J. Carroll, W. L. Wilson and L. E. Brus, J. Chem. Phys., 96, 946-954, (1992).

[8] Y. Shirai, A. J. Osgood, Y. Zhao, K. F. Kelly and J. M. Tour, Nano Lett., 5, 2330-2334, (2005).

[9] S. M. G. Risal Singh, Introduction to Nanotechnology, OXFORD University Press, (2016).

[10] L. A. Kolahalam, I. V. Kasi Viswanath, B. S. Diwakar, B. Govindh, V. Reddy and Y. L. N. Murthy, Mater. Today:. Proc., 18, 2182-2190, (2019).

[11] M. Steinhart, Angew. Chem. Int. Ed., 43, 2196-2197, (2004).

[12] J. L. Moran-Lopez, J. M. Sanchez (Eds.), Advanced Topics in Materials Science and Engineering, Springer US, (1993).

[13] A. Alshammari, V. N. Kalevaru and A. Martin, Catalysts, 6, 97, (2016).

[14] V. Polshettiwar and R. S. Varma, Green. Chem., 12, 743-754, (2010).

[15] N. Wang, S. Zeng, H. Yuan and J. Huang, J. Environ. Sci., 92, 1-10, (2020).

[16] H. Huo, Y. Jiang, T. Zhao, Z. Wang, Y. Hu, X. Xu and K. Lin, J. Mater. Sci., 55, 1475-1488, (2020).

[17] Y. Ren, K. Tang, W. Zhan, J. Luo and M. Wang, J. Alloys Compd., 821, 153427, (2020).

[18] C. Chen, C. Liang, J. Xu, J. Wei, X. Li, Y. Zheng, J. Li, H. Tang and J. Li, Electrochim. Acta, 335, 135708, (2020).

[19] Y.-X. Liu, S. Ohhashi, S. Kameoka and A. P. Tsai, Chem. Eng. Sci., 211, 115249, (2020).

[20] D. Mao, M. Jia, J. Qiu, X.-F. Zhang and J. Yao, Catal. Lett., 150, 74-81, (2020).

[21] Y. Xiong, Y. Ma, L. Zou, S. Han, H. Chen, S. Wang, M. Gu, Y. Shen, L. Zhang, Z. Xia, J. Li and H. Yang, J. Catal., 382, 247-255, (2020).

[22] K. Ham, S. Chung and J. Lee, J. Power Sources, 450, 227650, (2020).

[23] W. Gao, T. Liu, Z. Zhang, M. Dou and F. Wang, J. Mater. Chem. A, 8, 5525-5534, (2020).

[24] P. Puthiaraj, K. Yu, W.-S. Ahn and Y.-M. Chung, J. Ind. Eng. Chem., 81, 375-384, (2020).

[25] R. L. Oliveira, J. Kerstien, R. Schomäcker and A. Thomas, Catal. Sci. Technol., 10, 1385-1394, (2020).

[26] V. V. Karve, D. T. Sun, O. Trukhina, S. Yang, E. Oveisi, J. Luterbacher and W. L. Queen, Green. Chem., 22, 368-378, (2020).

[27] G. Garg, S. Foltran, I. Favier, D. Pla, Y. Medina-González and M. Gómez, Catal. Today, 346, 69-75, (2020).

[28] M. López-Viveros, I. Favier, M. Gómez, J.-F. Lahitte and J.-C. Remigy, Catal. Today, (2020).

[29] T. A. G. Duarte, I. Favier, C. Pradel, L. M. D. R. S. Martins, A. P. Carvalho, D. Pla and M. Gómez, ChemCatChem, 12, 2295-2303, (2020).

[30] A. Majeed, X. Li, P.-X. Hou, H. Tabassum, L. Zhang, C. Liu and H.-M. Cheng, Appl. Catal., B, 269, 118823, (2020).

[31] A. L. A. Marinho, R. C. Rabelo-Neto, F. Epron, N. Bion, F. S. Toniolo and F. B. Noronha, Appl. Catal., B, 268, 118387, (2020).

[32] Y. Qu, G. Xu, J. Yang and Z. Zhang, Appl. Catal., A, 590, 117311, (2020).

[33] J. S. DuChene, G. Tagliabue, A. J. Welch, X. Li, W.-H. Cheng and H. A. Atwater, Nano Lett., (2020).

[34] Q.-L. Hu, Z.-X. Zhang, J.-J. Zhang, S.-M. Li, H. Wang and J.-X. Lu, ACS Omega, 5, 3498-3503, (2020).

[35] S. Hejazi, S. Mohajernia, Y. Wu, P. Andryskova, G. Zoppellaro, I. Hwang, O. Tomanec, R. Zboril and P. Schmuki, Electrochem. Commun., 98, 82-86, (2019).

[36] A. Ahmed, M. Usman, B. Yu, X. Ding, Q. Peng, Y. Shen and H. Cong, J. Photochem. Photobiol., B, 202, 111682, (2020).

[37] A. Goswami, R. G. Kadam, J. Tuček, Z. Sofer, D. Bouša, R. S. Varma, M. B. Gawande and R. Zbořil, Chem. Eng. J., 382, 122469, (2020).

[38] Y. Yu, M. Zhai and J. Hu, Prog. Nat. Sci.: Mater. Int., 29, 511-516, (2019).

[39] Y. Shang, X. Xu, Q. Yue, B. Gao and Y. Li, Environ. Sci.: Nano, (2020).

[40] T. Wakisaka, K. Kusada, D. Wu, T. Yamamoto, T. Toriyama, S. Matsumura and H. Kitagawa, Chem. Lett., 49, 207-209, (2019).

[41] Y. Shi, G. Ji, Q. Hu, Y. Lu, X. Hu, B. Zhu and W. Huang, New J. Chem., 44, 20-23, (2020).

[42] M. Gopiraman, S. Saravanamoorthy, S. Ullah, A. Ilangovan, I. S. Kim and I. M. Chung, RSC Adv., 10, 2545-2559, (2020).

[43] J. Zhao, W. Y. Hernández, W. Zhou, Y. Yang, E. I. Vovk, M. Capron and V. Ordomsky, ChemCatChem, 12, 238-247, (2020).

[44] A. M. Abdel-Mageed, K. Wiese, M. Parlinska-Wojtan, J. Rabeah, A. Brückner and R. J. Behm, Appl. Catal., B, 118846, (2020).

[45] H. Ozay, P. Ilgin, M. K. Sezgintürk and O. Ozay, Int. J. Hydrogen Energy, 45, 9892-9902, (2020).

[46] M. Lashanizadegan, M. Anafcheh, H. Mirzazadeh and P. Gholipoor, Mater. Res. Bull., 125, 110773, (2020).

[47] Z. Chen, E. Vorobyeva, S. Mitchell, E. Fako, M. A. Ortuño, N. López, S. M. Collins, P. A. Midgley, S. Richard, G. Vilé and J. Pérez-Ramírez, Nat. Nanotechnol., 13, 702-707, (2018).

[48] H. Yu, Y. Xue, B. Huang, L. Hui, C. Zhang, Y. Fang, Y. Liu, Y. Zhao, Y. Li, H. Liu and Y. Li, iScience, 11, 31-41, (2019).

[49] X.-F. Yang, A. Wang, B. Qiao, J. Li, J. Liu and T. Zhang, Acc. Chem. Res., 46, 1740-1748, (2013).

[50] N. A. Hamill, C. Hardacre and S. E. J. McMath, Green. Chem., 4, 139-142, (2002).

[51] Y. Li and M. A. El-Sayed, J. Phys. Chem. B, 105, 8938-8943, (2001).

[52] R. R. Deshmukh, R. Rajagopal and K. V. Srinivasan, Chem. Commun., 1544-1545, (2001).

[53] R. Jin, Nanoscale, 7, 1549-1565, (2015).

[54] I. Favier, E. Teuma and M. Gómez, C.R. Chim., 12, 533-545, (2009).

[55] I. Favier, D. Madec, E. Teuma and M. Gomez, Curr. Org. Chem., 15, 3127-3174, (2011).

[56] I. Favier, D. Pla and M. Gómez, Chem. Rev., 120, 1146-1183, (2020).

[57] S. Klingelhöfer, W. Heitz, A. Greiner, S. Oestreich, S. Förster and M. Antonietti, J. Am. Chem. Soc., 119, 10116-10120, (1997).

[58] A. B. R. Mayer, J. E. Mark and S. H. Hausner, J. Appl. Polym. Sci., 70, 1209-1219, (1998).

[59] J. Le Bars, U. Specht, J. S. Bradley and D. G. Blackmond, Langmuir, 15, 7621-7625, (1999).

[60] J. H. Ding and D. L. Gin, Chem. Mater., 12, 22-24, (2000).

[61] W. Tu and H. Liu, Chem. Mater., 12, 564-567, (2000).

[62] Y. Li, E. Boone and M. A. El-Sayed, Langmuir, 18, 4921-4925, (2002).

[63] R. Narayanan and M. A. El-Sayed, J. Am. Chem. Soc., 125, 8340-8347, (2003).

[64] Ö. Metin, Ş. Şahin and S. Özkar, Int. J. Hydrogen Energy, 34, 6304-6313, (2009).

[65] Q. Yuan, J. Zhuang and X. Wang, Chem. Commun., 6613-6615, (2009).

[66] H. Erdoğan, Ö. Metin and S. Özkar, Phys. Chem. Chem. Phys., 11, 10519-10525, (2009).

[67] P. S. Roy, J. Bagchi and S. K. Bhattacharya, Colloids Surf. A Physicochem. Eng. Asp., 359, 45-52, (2010).

[68] M. Rakap, E. E. Kalu and S. Özkar, Int. J. Hydrogen Energy, 36, 1448-1455, (2011).

[69] Ö. Metin, F. Durap, M. Aydemir and S. Özkar, J. Mol. Catal. A: Chem., 337, 39-44, (2011).

[70] N. Naresh, F. G. S. Wasim, B. P. Ladewig and M. Neergat, J. Mol. Catal. A: Chem., 1, 8553-8559, (2013).

[71] M. Tamura and H. Fujihara, J. Am. Chem. Soc., 125, 15742-15743, (2003).

[72] S. U. Son, Y. Jang, K. Y. Yoon, E. Kang and T. Hyeon, Nano Lett., 4, 1147-1151, (2004).

[73] S. Jansat, M. Gómez, K. Philippot, G. Muller, E. Guiu, C. Claver, S. Castillón and B. Chaudret, J. Am. Chem. Soc., 126, 1592-1593, (2004).

[74] E. G. Mednikov, N. K. Eremenko, Y. L. Slovokhotov, Y. T. Struchkov and S. P. Gubin, J. Organomet. Chem., 258, 247-255, (1983).

[75] M. Zhao and R. M. Crooks, Angew. Chem. Int. Ed., 38, 364-366, (1999).

[76] V. Chechik and R. M. Crooks, J. Am. Chem. Soc., 122, 1243-1244, (2000).

[77] R. M. Crooks, M. Zhao, L. Sun, V. Chechik and L. K. Yeung, Acc. Chem. Res., 34, 181-190, (2001).

[78] R. Andrés, E. de Jesús and J. C. Flores, New J. Chem., 31, 1161-1191, (2007).

[79] J. C. Garcia-Martinez, R. W. J. Scott and R. M. Crooks, J. Am. Chem. Soc., 125, 11190-11191, (2003).

[80] T. Thurn-Albrecht, G. Meier, P. Müller-Buschbaum, A. Patkowski, W. Steffen, G. Grübel, D. L. Abernathy, O. Diat, M. Winter, M. G. Koch and M. T. Reetz, Phys. Rev. E, 59, 642-649, (1999).

[81] N. R. Jana, Z. L. Wang and T. Pal, Langmuir, 16, 2457-2463, (2000).

[82] Y. Piao, Y. Jang, M. Shokouhimehr, I. S. Lee and T. Hyeon, Small, 3, 255-260, (2007).

[83] M. T. Reetz, R. Breinbauer and K. Wanninger, Tetrahedron Lett., 37, 4499-4502, (1996).

[84] M. Beller, H. Fischer, K. Kühlein, C. P. Reisinger and W. A. Herrmann, J. Organomet. Chem., 520, 257-259, (1996).

[85] M. T. Reetz, M. Winter and B. Tesche, Chem. Commun., 147-148, (1997).

[86] M. T. Reetz and E. Westermann, Angew. Chem. Int. Ed., 39, 165-168, (2000).

[87] M. Jin, H. Liu, H. Zhang, Z. Xie, J. Liu and Y. Xia, Nano Res., 4, 83-91, (2011).

[88] A. Troupis, A. Hiskia and E. Papaconstantinou, Angew. Chem. Int. Ed., 41, 1911-1914, (2002).

[89] J. Zhang, B. Keita, L. Nadjo, I. M. Mbomekalle and T. Liu, Langmuir, 24, 5277-5283, (2008).

[90] A. Corma, S. Iborra, F. X. Llabrés i Xamena, R. Montón, J. J. Calvino and C. Prestipino, J. Phys. Chem. C, 114, 8828-8836, (2010).

[91] B. Riflade, J. Oble, L. Chenneberg, E. Derat, B. Hasenknopf, E. Lacôte and S. Thorimbert, Tetrahedron, 69, 5772-5779, (2013).

[92] L. D’Souza, M. Noeske, R. M. Richards and U. Kortz, J. Colloid Interface Sci., 394, 157-165, (2013).

[93] L. D'Souza, M. Noeske, R. M. Richards and U. Kortz, Appl. Catal., A, 453, 262-271, (2013).

[94] L. Hong, Y. Gui, J. Lu, J. Hu, J. Yuan and L. Niu, Int. J. Hydrogen Energy, 38, 11074-11079, (2013).

[95] J. M. Cameron, J. Gao, D.-L. Long and L. Cronin, Inorg. Chem. Front., 1, 178-185, (2014).

[96] D. Kim, J. H. Seog, M. Kim, M. Yang, E. Gillette, S. B. Lee and S. W. Han, Chem. Eur. J., 21, 5387-5394, (2015).

[97] R. Villanneau, A. Roucoux, P. Beaunier, D. Brouri and A. Proust, RSC Adv., 4, 26491-26498, (2014).

[98] X. Xie, Y. Nie, S. Chen, W. Ding, X. Qi, L. Li and Z. Wei, J. Mater. Chem., 3, 13962-13969, (2015).

[99] L. Chen, T. Feng, P. Wang, Z. Chen, R. Yan, B. Liao and Y. Xiang, Appl. Catal., A, 523, 304-311, (2016).

[100] Y. Zhang, H. Wang, Q. Yao, F. Yan, C. Cui, M. Sun and H. Zhang, RSC Adv., 6, 39618-39626, (2016).

[101] J. H. Seog, D. Kim, Y. Kim, N. S. Kim, S. B. Lee and S. Woo Han, CrystEngComm, 18, 6029-6034, (2016).

[102] J. Hu, X. Wu, Q. Zhang, M. Gao, H. Qiu, K. Huang, S. Feng, Y. Yang, Z. Liu and B. Zhao, Electrochem. Commun., 83, 56-60, (2017).

[103] X. Kong, Y. Wang, Q. Zhang, T. Zhang, Q. Teng, L. Wang, H. Wang and Y. Zhang, J. Colloid Interface Sci., 505, 615-621, (2017).

[104] Y. Leng, C. Zhang, B. Liu, M. Liu, P. Jiang and S. Dai, ChemSusChem, 11, 3396-3401, (2018).

[105] L. Wang, T. Meng, J. Sun, S. Wu, M. Zhang, H. Wang and Y. Zhang, Anal. Chim. Acta, 1047, 28-35, (2019).

[106] M. T. Reetz and M. Maase, Adv. Mater., 11, 773-777, (1999).

[107] S. Chen, K. Huang and J. A. Stearns, Chem. Mater., 12, 540-547, (2000).

[108] E. Sadeghmoghaddam, C. Lam, D. Choi and Y.-S. Shon, J. Mater. Chem., 21, 307-312, (2011).

[109] G. Schmid, M. Harms, J. O. Malm, J. O. Bovin, J. Van Ruitenbeck, H. W. Zandbergen and W. T. Fu, J. Am. Chem. Soc., 115, 2046-2048, (1993).

[110] C. Amiens, D. de Caro, B. Chaudret, J. S. Bradley, R. Mazel and C. Roucau, J. Am. Chem. Soc., 115, 11638-11639, (1993).

[111] I. I. Moiseev, T. A. Stromnova and M. N. Vargaftik, J. Mol. Catal., 86, 71-94, (1994).

[112] M. Moreno-Mañas, R. Pleixats and S. Villarroya, Organometallics, 20, 4524-4528, (2001).

[113] J. Walter, Adv. Mater., 12, 31-33, (2000).

[114] J. Walter, J. Heiermann, G. Dyker, S. Hara and H. Shioyama, J. Catal., 189, 449-455, (2000).

[115] K. Fukaya and T. Yamase, Angew. Chem., 115, 678-682, (2003).

[116] N. Narkhede, S. Singh and A. Patel, Green. Chem., 17, 89-107, (2015).

[117] D.-Y. Du, J.-S. Qin, S.-L. Li, Z.-M. Su and Y.-Q. Lan, Chem. Soc. Rev., 43, 4615-4632, (2014).

[118] Y. Ren, M. Wang, X. Chen, B. Yue and H. He, Materials, 8, (2015).

[119] J. M. Clemente-Juan, E. Coronado and A. Gaita-Ariño, Chem. Soc. Rev., 41, 7464-7478, (2012).

[120] O. Oms, A. Dolbecq and P. Mialane, Chem. Soc. Rev., 41, 7497-7536, (2012).

[121] H. Wang, S. Hamanaka, Y. Nishimoto, S. Irle, T. Yokoyama, H. Yoshikawa and K. Awaga, J. Am. Chem. Soc., 134, 4918-4924, (2012).

[122] M. Ammam and J. Fransaer, J. Electrochem. Soc., 158, A14-A21, (2011).

[123] M. Kourasi, R. G. A. Wills, A. A. Shah and F. C. Walsh, Electrochim. Acta, 127, 454-466, (2014).

[124] B. Keita and L. Nadjo, J. Mol. Catal. A: Chem., 262, 190-215, (2007).

[125] Y. Ren, B. Yue, M. Gu and H. He, Materials, 3, (2010).

[126] A. Dolbecq, E. Dumas, C. R. Mayer and P. Mialane, Chem. Rev., 110, 6009-6048, (2010).

[127] H. Lv, Y. V. Geletii, C. Zhao, J. W. Vickers, G. Zhu, Z. Luo, J. Song, T. Lian, D. G. Musaev and C. L. Hill, Chem. Soc. Rev., 41, 7572-7589, (2012).

[128] R. Sivakumar, J. Thomas and M. Yoon, J. Photochem. Photobiol., 13, 277-298, (2012).

[129] Y. Wang and I. A. Weinstock, Chem. Rev., 41, 7479-7496, (2012).

[130] P. Yin, D. Li and T. Liu, Chem. Rev., 41, 7368-7383, (2012).

[131] Michael T. Pope, M. Sadakane and U. Kortz, Eur. J. Inorg. Chem., 2019, 340-342, (2019).

[132] J. F. Keggin, Nature, 131, 908-909, (1933).

[133] J. F. Keggin and L. Bragg William, Proceedings of the Royal Society of London. Series A, Containing Papers of a Mathematical and Physical Character, 144, 75-100, (1934).

[134] N. Mizuno and M. Misono, Chem. Rev., 98, 199-218, (1998).

[135] V. Kogan, Z. Aizenshtat, R. Popovitz-Biro and R. Neumann, Org. Lett., 4, 3529-3532, (2002).

[136] L. Chalkley, J. Phys. Chem., 56, 1084-1086, (1952).

[137] K. Mori, K. Furubayashi, S. Okada and H. Yamashita, RSC Adv., 2, 1047-1054, (2012).

[138] K. A. San and Y.-S. Shon, Nanomaterials, 8, 346, (2018).

[139] P. Migowski, K. Luska, W. Leitner and M. Prechtl. Nanocatalysis in Ionic Liquids. Wiley-VCH, Weinheim; 2017.

[140] J. M. Patete, X. Peng, C. Koenigsmann, Y. Xu, B. Karn and S. S. Wong, Green. Chem., 13, 482-519, (2011).

[141] F. Fiévet, S. Ammar-Merah, R. Brayner, F. Chau, M. Giraud, F. Mammeri, J. Peron, J. Y. Piquemal, L. Sicard and G. Viau, Chem. Soc. Rev., 47, 5187-5233, (2018).

[142] I. Favier, D. Pla and M. Gómez, Catal. Today, 310, 98-106, (2018).

[143] R. Fehrmann, A. Riisager and M. Haumann, Supported Ionic Liquids: Fundamentals and Applications, Wiley, (2014).

[144] J. Schwartz, Acc. Chem. Res., 18, 302-308, (1985).

[145] J. A. Anderson and M. F. Garcia, Supported Metals in Catalysis, Imperial College Press, (2012).

[146] G. M. Maksimova, A. L. Chuvilin, E. M. Moroz, V. A. Likholobov and K. I. Matveev, Kinet. Catal., 45, 870-878, (2004).

[147] P. Kishore, B. Viswanathan and T. Varadarajan, Nanoscale Res. Lett., 3, 14, (2007).

[148] J. Chevalier, L. Gremillard, A. V. Virkar and D. R. Clarke, J. Am. Ceram. Soc., 92, 1901-1920, (2009).

[149] A. Suresh, M. J. Mayo, W. D. Porter and C. J. Rawn, J. Am. Ceram. Soc., 86, 360-362, (2003).

[150] K. Muto, J. Yamaguchi, D. G. Musaev and K. Itami, Nat. Commun., 6, 7508, (2015).

[151] A. Fawcett, T. Biberger and V. K. Aggarwal, Nat. Chem., 11, 117-122, (2019).

[152] C. C. C. Johansson Seechurn, M. O. Kitching, T. J. Colacot and V. Snieckus, Angew. Chem. Int. Ed., 51, 5062-5085, (2012).

[153] K. Kubota, T. Seo, K. Koide, Y. Hasegawa and H. Ito, Nat. Commun., 10, 111, (2019).

[154] T. Mizoroki, K. Mori and A. Ozaki, Bull. Chem. Soc. Jpn., 44, 581-581, (1971).

[155] K. Mori, T. Mizoroki and A. Ozaki, Bull. Chem. Soc. Jpn., 46, 1505-1508, (1973).

[156] R. F. Heck and J. P. Nolley, J. Org. Chem., 37, 2320-2322, (1972).

[157] H. A. Dieck and R. F. Heck, J. Am. Chem. Soc., 96, 1133-1136, (1974).

[158] J. M. Thomas and W. J. Thomas, Principles and practice of heterogeneous catalysis, VCH, (1997).

[159] R. A. van Santen, B. A. Averill, J. A. Moulijn and P. W. N. M. van Leeuwen, Catalysis: An Integrated Approach, Elsevier Science, (2000).

[160] R. Richards, Surface and Nanomolecular Catalysis, CRC Press, (2006).

[161] D. A. Skoog, F. J. Holler and T. A. Nieman, Principles of Instrumental Analysis, Saunders College Pub., (1998).

[162] J. H. Clark, A. P. Kybett and D. J. Macquarrie, Supported Reagents: Preparation, Analysis, and Applications, Wiley, (1992).

[163] J. Klinowski and O. N. Antzutkin, New Techniques in Solid-State NMR, Springer, (2004).

[164] D. Briggs, Surf. Interface Anal., 3, v-v, (1981).

[165] J. C. H. Spence, High-Resolution Electron Microscopy, OUP Oxford, (2013).

[166] A. Muller and J. Grazul, J. Electron Microsc., 50, 219-226, (2001).

[167] P. Ferreira, I. M. Fonseca, A. M. Ramos, J. Vital and J. E. Castanheiro, Appl. Catal., B, 98, 94-99, (2010).

[168] P. Vázquez, L. Pizzio, C. Cáceres, M. Blanco, H. Thomas, E. Alesso, L. Finkielsztein, B. Lantaño, G. Moltrasio and J. Aguirre, J. Mol. Catal. A: Chem., 161, 223-232, (2000).

[169] D. L. Pavia, G. M. Lampman, G. S. Kriz and R. G. Engel, Introduction to Organic Laboratory Techniques: A Small Scale Approach, Thomson Brooks/Cole, (2005).